frontiers in Microbiology

TYPE Original Research
PUBLISHED 21 September 2026
DOI 10.3389/fmicb.2026.1924276

Check for updates

OPEN ACCESS

EDITED BY
Thi Thu Hoai Nguyen,
Vietnam National University, Vietnam

REVIEWED BY
Ganesh Kumar Maurya,
Banaras Hindu University, India
Maria Gabriela Vela Chauvin,
Universidad San Francisco de Quito, Ecuador
Joshua James Iszatt,
University of Western Australia, Australia

*CORRESPONDENCE
Sandra Sevilla-Navarro
✉ s.sevilla@cecav.org

RECEIVED 30 June 2026
REVISED 30 July 2026
ACCEPTED 10 August 2026
PUBLISHED 21 September 2026

CITATION
Garcia-Llorens J, Gómez-Cano IS, Torres-Boncompte J, Soriano JM, Catalá-Gregori P and Sevilla-Navarro S (2026) Quantitative phage-host interaction profiling supports the design of a broadly active phage cocktail against multidrug-resistant *Enterococcus faecalis* from poultry. *Front. Microbiol.* 17:1924276. doi: 10.3389/fmicb.2026.1924276

COPYRIGHT
© 2026 Garcia-Llorens, Gómez-Cano, Torres-Boncompte, Soriano, Catalá-Gregori and Sevilla-Navarro. This is an open-access article distributed under the terms of the Creative Commons Attribution License (CC BY). The use, distribution or reproduction in other forums is permitted, provided the original author(s) and the copyright owner(s) are credited and that the original publication in this journal is cited, in accordance with accepted academic practice. No use, distribution or reproduction is permitted which does not comply with these terms.

Quantitative phage-host interaction profiling supports the design of a broadly active phage cocktail against multidrug-resistant *Enterococcus faecalis* from poultry

Josep Garcia-Llorens[1,2], Ignacio Samuel Gómez-Cano[1], Jan Torres-Boncompte[1], Jose M. Soriano[2,3], Pablo Catalá-Gregori[1,4] and Sandra Sevilla-Navarro[1,4]*

[1]Centro de Calidad Avícola y Alimentación Animal de la Comunidad Valenciana, (CECAV), Castellón, Spain, [2]Food & Health Lab, Institute of Materials Science, University of Valencia, Valencia, Spain, [3]Joint Research Unit on Endocrinology, Nutrition and Clinical Dietetics, University of Valencia-Health Research Institute La Fe, Valencia, Spain, [4]Departamento de Producción y Sanidad Animal, Salud Pública Veterinaria y Ciencia y Tecnología de los Alimentos, Instituto de Ciencias Biomédicas, Facultad de Veterinaria, Universidad Cardenal Herrera-CEU, CEU Universities, Moncada, Spain

Introduction: *Enterococcus faecalis* is an opportunistic pathogen of One Health relevance and an important reservoir of antimicrobial resistance in poultry production systems. In this study, we generated a large-scale quantitative phage-host interaction dataset to support the rational design of phage cocktails targeting multidrug-resistant poultry-associated *E. faecalis*.
Methods: Thirty-eight lytic phages were isolated from poultry farm samples, genomically characterized, and evaluated against 51 clinical poultry isolates using efficiency of plating as a quantitative measure of productive infectivity.
Results: The complete phage collection achieved 94.12% cumulative strain coverage, while genomic relatedness showed only a moderate association with infectivity profiles, highlighting the need for functional screening. Computational optimization identified a six-phage cocktail, CKT6, which displayed broad *in vitro* activity against diverse strain backgrounds, reaching 92.16% coverage at MOI 1. Importantly, cocktail performance was not fully predictable from individual phage activity, as host-dependent synergistic and antagonistic effects were observed.
Discussion: These findings support quantitative phage-host interaction profiling as a robust framework for reproducible and adaptive phage-cocktail design. Further validation under biofilm-associated, formulation-relevant and field-like poultry-production conditions will be required before practical application.

KEYWORDS
antimicrobial resistance, *Enterococcus*, genomic analysis, host range, phage therapy, poultry production

1 Introduction

Enterococcus spp. are widely distributed in the environment and are recognized as important opportunistic pathogens in both humans and animals (Byappanahalli et al., 2012). Among them, *Enterococcus faecalis* (*E. faecalis*) stands out for its ability to express multiple virulence factors, including biofilm formation and cytolysin production, which promote colonization, persistence, and tissue damage (Reynolds et al., 2025). In poultry, this pathogenic potential is well documented, as *E. faecalis* is associated with a wide range of disease conditions, including septicaemia, endocarditis, arthritis, and spondylitis, leading to significant economic losses due to increased mortality and reduced productivity across different production systems (Stępień-Pyśniak et al., 2016; Nielsen et al., 2022; Bzdil et al., 2023).

Beyond poultry production, *E. faecalis* is also of considerable clinical relevance in humans. Human enterococcal infections commonly include urinary tract infections, bacteraemia, infective endocarditis, and wound or intra-abdominal infections, and their treatment is often complicated by intrinsic resistance to several antimicrobial classes as well as the ability to acquire and disseminate additional resistance determinants [Centers for Disease Control and Prevention (CDC), 2024; Said et al., 2024]. From a One Health perspective, this connection between human and poultry-associated *E. faecalis* is particularly relevant, as enterococci are frequently detected in poultry meat, and chicken-associated isolates may display multidrug resistance, virulence traits, and genetic relatedness to lineages of clinical concern (Bortolaia et al., 2016). Controlling *E. faecalis* at the poultry-production level may have implications beyond animal health, contributing to the reduction of potential reservoirs of resistant enterococci and resistance genes along the food chain (Poulsen et al., 2012).

The rising prevalence of antimicrobial resistance (AMR) in *E. faecalis* represents a major challenge in poultry production, as it compromises both disease control and treatment effectiveness (Jung et al., 2018). The rise of resistance significantly reduces available therapeutic options and is associated with increased morbidity and mortality (Dupont et al., 2011; Garcia-Llorens et al., 2025). Moreover, treatment outcomes are often suboptimal, particularly when infections are not detected early, and are further hindered by the ability of *E. faecalis* to persist in biofilms and farm environments (Bzdil et al., 2023; Morishita, 2025; Reynolds et al., 2025). These factors not only impact animal health and productivity but also highlight the broader implications of AMR, including the potential risk of zoonotic transmission (Martinez-Laorden et al., 2023; Kerek et al., 2024). In this context, the limitations of conventional antimicrobials, combined with the lack of effective vaccines and broadly implemented prophylactic strategies, underscore the urgent need for alternative control strategies (Nielsen et al., 2022).

Bacteriophages, viruses that specifically infect bacteria, have emerged as promising biological tools for the control of multidrug-resistant pathogens (Lavilla et al., 2023). Their key advantages include high host specificity, the capacity to self-amplify at the site of infection, and a favourable safety profile (Kutter et al., 2010; Uyttebroek et al., 2022; Rodríguez-Lucas and Ladero, 2023), making them particularly attractive for application in complex environments such as poultry production systems. Accordingly, bacteriophages have gained considerable attention as a promising strategy for controlling *E. faecalis* in poultry systems and derived products (Rodríguez-Lucas and Ladero, 2023; Li et al., 2026). Despite the increasing interest in phage-based control strategies, the design of effective phage cocktails remains challenging due to the marked field-level diversity of *E. faecalis* and the limited predictability of phage host range. In particular, for poultry-associated *E. faecalis*, there is a lack of systematically generated, efficiency of plating (EOP)-based quantitative infectivity datasets across large and diverse clinical strain panels that could inform rational, computationally guided cocktail selection.

Thus, the present study addressed this gap by generating a large collection of phages and evaluating their activity against a diverse panel of clinical poultry isolates. To this end, quantitative infectivity data, genomic analyses, and computational optimization approaches were integrated to identify a broadly active phage cocktail against multidrug-resistant *E. faecalis*. Furthermore, phage-host interaction patterns were evaluated to determine their utility for the rational design of robust phage cocktails.

2 Materials and methods

2.1 Bacterial strains and culture conditions

A total of 51 clinical *E. faecalis* strains were included in this study. These isolates originated from the collection previously described by Garcia-Llorens et al. (2025), which comprised strains recovered from different poultry farms across Spain, providing broad national representation. Strains were selected based on production system (layers, breeders, and broilers), virulence profiles, and multidrug resistance characteristics.

All strains were reactivated by triple streaking on Columbia Blood Agar (CA) (Oxoid Deutschland GmbH, Wesel, Germany) plates and incubated overnight (ON) at 37.5 °C. The resulting cultures were subsequently stored at 4 °C for further analyses.

2.2 Source of phage isolation

Phages were isolated from poultry samples (including faeces, cloacal swabs, drag swabs and litter) collected from commercial poultry farms over a one-year period (2024) as part of the laboratory's routine diagnostic workflow.

Environmental samples were diluted 1:10 (w/v) in buffered peptone water (BPW, VWR Chemicals, Barcelona, Spain) and incubated ON at 37 °C. Following incubation, 1 mL of each sample was pooled in groups of 10 samples, used as starting material for phage isolation.

2.3 Phage isolation, purification and propagation

Samples were centrifuged 8,000 × *g* for 5 min and the supernatant was subsequently filtered through a 0.22 µm pore size polyether sulfone (PES) membrane filter (VWR Chemicals, Barcelona, Spain) to remove any remaining bacteria. To evaluate the lytic potential of the filtered samples, a spot test assay was employed against the *E. faecalis* strains (Mirzaei and Nilsson, 2015). Samples demonstrating clear lytic activity were selected for phage isolation procedures. Each lysate was serially diluted 1:10 in LB broth (Scharlau, Barcelona, Spain) and mixed with 200 µL of the exponential-phase of host bacterial suspension at an optical density at 600 nm (OD_{600}) of 0.4 (~10^8 CFU/mL). Following an incubation of 15 min period at room

temperature to allow phage adsorption, the mixture was incorporated into 5 mL of LB soft agar (0.6% agar; Scharlau, Barcelona, Spain) and overlaid onto LB agar (Scharlau, Barcelona, Spain) plates using the double-layer agar (DLA) (Mirzaei and Nilsson, 2015). Plates were incubated at 37 °C, ON. This purification cycle was repeated three times, until a single purified phage isolate was obtained. Whenever a phage was isolated against a particular strain, it was subsequently evaluated by spot assay against the remaining strains. This process was repeated until a phage collection with coverage of all 51 strains was established.

2.4 Host range (HR) and efficiency of plating (EOP)

Host range (HR) was first assessed as a qualitative screening to identify phage-strain combinations showing lytic activity against the propagation strains and the complete panel of challenge *E. faecalis* strains ($n = 51$). Lytic reactions were recorded according to plaque/lysis appearance, and only combinations showing clear lysis (C) were further evaluated by efficiency of plating (EOP), in order to focus on productive infections and avoid overestimating host range based on non-productive lysis or growth inhibition (Kutter, 2009). For EOP determination, serial 1:10 dilutions of the purified phages were carried out, and each dilution was tested through the DLA method. After an ON incubation at 37 °C, both lytic activity and phage titers capabilities were determined. EOP towards the strains was calculated relative to titers the phage reached with its own propagation strains, only when clear and individual plaques were observed (Torres-Boncompte et al., 2025).

2.5 Rational design of phage cocktails

Phage-cocktail formulation was based on the experimental assessment of phage lytic activity determined by EOP. EOP values obtained against the tested bacterial strains were classified according to lytic efficiency as follows: values ≥0.5 were considered indicative of high lytic efficiency; values between 0.2 and <0.5 as moderate lytic activity; values between 0.001 and <0.2 as low lytic efficiency; and values <0.001 as non-lytic. Accordingly, EOP values below 0.5 were regarded as suboptimal lytic efficiency, and the absence of lysis was recorded as zero lytic activity, following established EOP based phage efficacy assessment criteria (Panteleev et al., 2025).

Based on these EOP results, binary HR matrices were constructed by assigning a value of 1 to phage-strain combinations exhibiting productive lytic activity and 0 to those showing no detectable lysis. These HR matrices were used as input for the computational optimization of phage cocktail composition.

Phage cocktail optimization was performed using the optimal set selection strategy described by Díaz-Galián et al. (2022), implemented through the ExhaustiveSearch algorithm of the PhageCocktail package within the R statistical environment (R Core Team, 2025). To avoid unnecessarily complex formulations and based on previous systematic analyses indicating that phage cocktails composed of a limited number of well characterized phages achieve an effective balance between host specificity, antibacterial potency, and formulation stability, the maximum size of the phage cocktail was constrained to seven phages (Molina et al., 2022).

Phages selected by the computational optimization algorithm for cocktail formulation were subsequently subjected to more extensive phenotypic and genotypic characterization, together with a detailed evaluation of their efficacy against clinical *E. faecalis* strains.

2.6 Genomic characterization

Phage DNA was extracted from previously purified lysates. Aliquots of 500 µL of each lysate were treated with nucleases to remove residual host DNA and RNA. To this end, each sample was treated with 1.25 µL of DNase I (Applied Biosystems), along with 1.25 µL of RNase A (Omega Biotek), and incubated at 37 °C for 1 h 30 min. The nuclease reaction was stopped by adding 25 µL of 0.4 M EDTA, followed by incubation at 75 °C for 1 h. Subsequently, 20 µL of proteinase K (20 mg/mL) was added, and samples were incubated at 55 °C for 30 min. DNA was then purified using the Quick-DNA/RNA Viral Kit (Zymo Research) according to the manufacturer's instructions.

Phage genomic sequencing was performed using Oxford Nanopore Technologies. Basecalled FASTQ reads were processed independently for each phage isolate. Read quality was assessed with NanoPlot v1.46.2 to inspect read length distribution, read quality scores and overall sequencing performance (De Coster and Rademakers, 2023). Reads were quality-filtered with Chopper v0.11.0 using a minimum read length of 500 bp and a minimum mean Phred quality score of 9 (De Coster and Rademakers, 2023). Filtered reads were assembled *de novo* with Flye v2.9.5 using the nano-hq option and five internal polishing iterations (Kolmogorov et al., 2019). Draft assemblies were further polished through five rounds of Racon v1.5.0 after read mapping with minimap2 v2.30 using the map-ont preset (Vaser et al., 2017; Li, 2018), followed by final polishing with Medaka v2.2.1 using the r941_min_sup_g507 model (Lee et al., 2021). Medaka-polished sequences were retained as the final assemblies for downstream analyses.

Genome quality and completeness were assessed using CheckV v1.0.3 with the CheckV database v1.5 and the end-to-end workflow (Nayfach et al., 2021). Structural and functional annotation was performed with Pharokka v1.8.1, with coding sequences predicted using PHANOTATE as implemented within Pharokka (McNair et al., 2019; Bouras et al., 2023). Annotated genomes were inspected to identify functional modules associated with DNA packaging, morphogenesis, host-cell lysis, DNA metabolism and other phage-related functions.

Taxonomic clustering of the phage genomes was performed through gene-sharing network analysis using vConTACT2 v0.11.3 (Jang et al., 2019). A custom reference database was generated from INPHARED by filtering entries to retain only phages reported to infect *Enterococcus* hosts (Cook and Hynes, 2025). The resulting network and genome overview table were inspected in Cytoscape v3.10.4 (Shannon et al., 2003), and the final figure was generated in R using the graph package.

For the six phages selected for the optimized cocktail (CKT6), taxonomic assignment at the genus and species levels was further assessed using taxMyPhage through the PhageCompass web service (Millard et al., 2025). Comparative genomic visualization was performed using clinker against RefSeq reference genomes representative of the corresponding predicted genera to assess genome organization and conserved functional modules (Gilchrist and Chooi, 2021). Intergenomic similarity was further assessed using VIRIDIC to calculate pairwise nucleotide-based genomic similarity, and using VirClust to calculate pairwise proteome-based similarity through shared

protein clusters (PCs), both against RefSeq reference genomes representative of the corresponding predicted genera.

Genomic safety and lifestyle prediction were assessed using complementary *in silico* tools. PhageLeads was used to evaluate therapeutic suitability and screen for markers associated with temperate lifestyle, antimicrobial resistance and virulence (Yukgehnaish et al., 2022). Additional screening for antimicrobial resistance, virulence-associated and plasmid-related sequences was performed using ABRicate (Seemann, 2016). Phage lifestyle was further evaluated using PhaTYP as implemented in the PhaBOX platform (Shang et al., 2023a, b). Tail-associated genomic regions were inspected to identify coding sequences (CDS) potentially involved in host recognition, and putative depolymerase enzymes were predicted using the DePolymerase Predictor (DePP, web version 1.0.0), considering proteins with a predicted probability greater than 90% as potential depolymerases (Magill and Skvortsov, 2023).

2.7 Phenotypic characterization of selected cocktail phages

Plaque morphology was recorded for each phage on its corresponding propagation strain, and plaque diameter was quantified (n = 10 plaques per phage). Virions were examined by transmission electron microscopy (TEM) at the Centro de Investigación Príncipe Felipe (CIPF, Valencia, Spain) using a Tecnai G2 Spirit BioTWIN microscope operated at 120 kV. Lysates (10^8–10^{10} PFU/mL) were first fixed in 2% (wt/vol) paraformaldehyde in aqueous solution, and 10 µL aliquots were applied onto carbon coated copper grids. After a 15 min adsorption period, grids were subjected to glow discharge at 7.2 kV, rinsed for 2 min in 0.1 M PBS, and post fixed in 1% (wt/vol) glutaraldehyde. Samples were negatively stained with 1% (wt/vol) uranyl acetate and subsequently contrasted in 1% (wt/vol) methyl cellulose for 30 s before air drying and storage until imaging. Phage morphotypes were assigned on the basis of virion architecture in TEM micrographs and classified according to current International Committee on Taxonomy of Viruses (ICTV) recommendations.

2.8 pH and temperature stability

Phage stability was evaluated under different pH and temperature conditions. For pH stability assays, high titer phage suspensions (>10^8 PFU/mL) were diluted 1:10 in buffered solutions adjusted to pH 2–12 and incubated at 37.5 °C for 2 h. Phage viability was determined by serial dilution and quantified using the drop plate method. Phages incubated at pH 7 were used as controls to calculate survival percentages. All assays were performed in triplicate (Torres-Boncompte et al., 2025).

Thermal stability was assessed by incubating 1:10 dilutions of phage stocks (>10^8 PFU/mL) in LB broth at 30–80 °C for 30 and 60 min. Following heat exposure, phage titers were determined by serial dilution and drop plate enumeration. Samples stored at 4 °C and −80 °C were used as controls to establish baseline stability (Torres-Boncompte et al., 2025).

2.9 Kinetics of infection of individual selected phages

Infection kinetics were assessed as described by Alrafaie et al. (2024) with slight modifications. In 96-well plates, 160 µL of LB together with 20 µL of the exponential-phase of host bacterial suspension (OD_{600} = 0.4) and 20 µL of phage suspension were added to achieve multiplicity of infection (MOI) of 10, 1, 0.1 and 0.01. OD_{600} measurements were taken every 5 min up to 12 h at 37 °C with continuous shaking using a microplate spectrophotometer (Multiskan SkyHigh, Thermo Fisher Scientific™). All the values obtained were later corrected with blank values.

2.10 One-step growth and burst size analysis

To estimate the latent period and burst size of the six phages selected for the CKT6 cocktail, one-step growth curves were performed based on the protocol previously reported by Torres-Boncompte et al. (2025). Briefly, host bacterial cultures were grown to exponential phase (OD_{600} = 0.4) and inoculated with each phage at a multiplicity of infection (MOI) of 0.1, allowing adsorption for 10 min at 37 °C. Following centrifugation to remove non-adsorbed phage particles, infected cells were resuspended in fresh LB broth. Aliquots were collected at defined time points and phage titers were determined by the double-layer agar (DLA) technique. Latent period was defined as the interval elapsed between infection and the beginning of the first progeny burst, whereas burst size was estimated by dividing the phage titer at the plateau phase by the number of bacterial cells initially infected. Aliquots were collected every 10 min over a 100 min period, and phage titers were determined by the double-layer agar (DLA) technique. Latent period was defined as the interval elapsed between infection and the beginning of the first progeny burst. Burst size was calculated according to the following formula: Burst size = (average phage titer at the plateau phase − average phage titer before the burst) / (number of infected bacterial cells); where the number of infected bacterial cells was estimated as the phage inoculum administered (MOI × initial bacterial concentration) minus the titer of non-adsorbed phages recovered in the supernatant after the 10-min centrifugation step. All titer values used in this calculation were expressed in PFU prior to $\log_{10}$ (PFU/mL) transformation for graphical representation. One-step growth curve experiments were performed in biological triplicate (n = 3) for each phage, and results are expressed as mean ± standard deviation.

2.11 *In vitro* efficacy of the optimized cocktail

The *in vitro* lytic activity of the optimized phage cocktail was assessed for all clinical *E. faecalis* strains using the previously described kinetic infection assay at a MOI of 1, including untreated bacterial controls. Lytic activity was determined by comparing the growth kinetics of phage-treated cultures with controls. All assays were performed at least in triplicate to ensure reproducibility.

2.12 Statistical analysis

Phage-host interaction analyses were performed using the EOP matrix obtained from host range assays. Phage-strain combinations with EOP values ≥ 0.5 were considered positive productive interactions. The association between genotypic relatedness and EOP-based infectivity profiles was assessed using a Mantel test with the vegan package. The genotypic distance matrix was compared with the phenotypic Bray–Curtis dissimilarity matrix calculated from quantitative

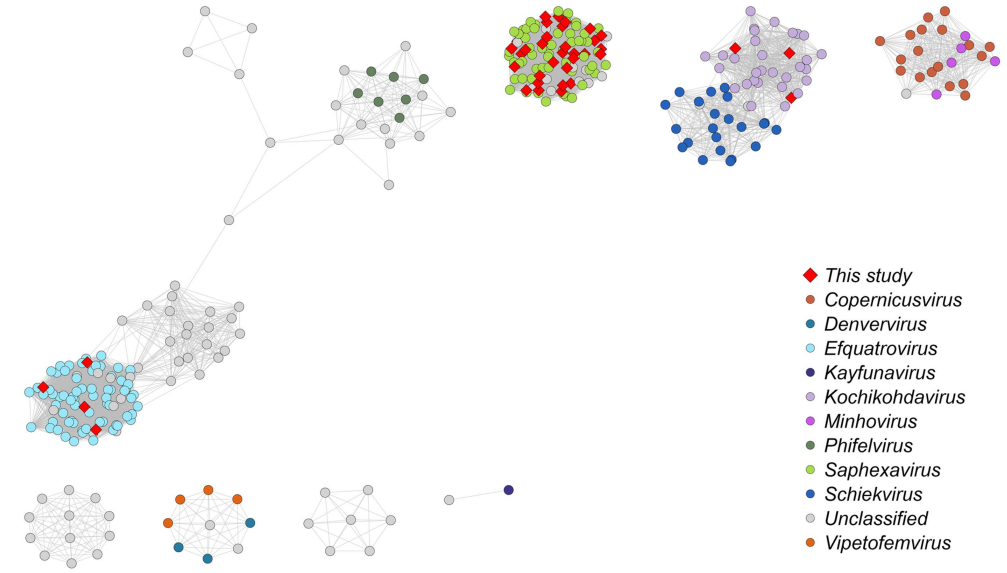


FIGURE 1
Gene-sharing network analysis of *Enterococcus* phages isolated in this study and related reference phages. The network was generated using vConTACT2 based on shared gene content. Red diamonds indicate phages isolated in this study, circles represent reference phages, node colours indicate genus-level taxonomic assignments, and grey nodes correspond to unclassified phages.

EOP values. Spearman's rank correlation coefficient was used, and significance was assessed using 9,999 unrestricted permutations (R Studio v.2026.04.).

Differences in lysis patterns among cocktails were analysed using cumulative link mixed models, considering lysis outcome as an ordinal variable (P < T < C). Complete lysis was further analysed as a binary outcome (C *vs.* T/P) using mixed-effects logistic regression, with cocktail formulation as a fixed effect and bacterial strain as a random effect. Pairwise comparisons were performed using estimated marginal means with Holm correction.

3 Results

3.1 Phage diversity and distribution across viral clusters

Extensive phage hunting was performed on poultry farm samples collected over a one-year period, using 51 *E. faecalis* strains as primary hosts. A total of 38 *E. faecalis* bacteriophages with demonstrated lytic activity were isolated from 880 pooled samples (equivalent to 8,800 individual field samples). Lytic activity characterization using the DLA method confirmed that the complete phage collection was capable of producing lytic activity against 94.12% (n = 48/51) of the tested *E. faecalis* strains, with only three strains showing either turbid lysis or no productive lysis (Supplementary Figure 1).

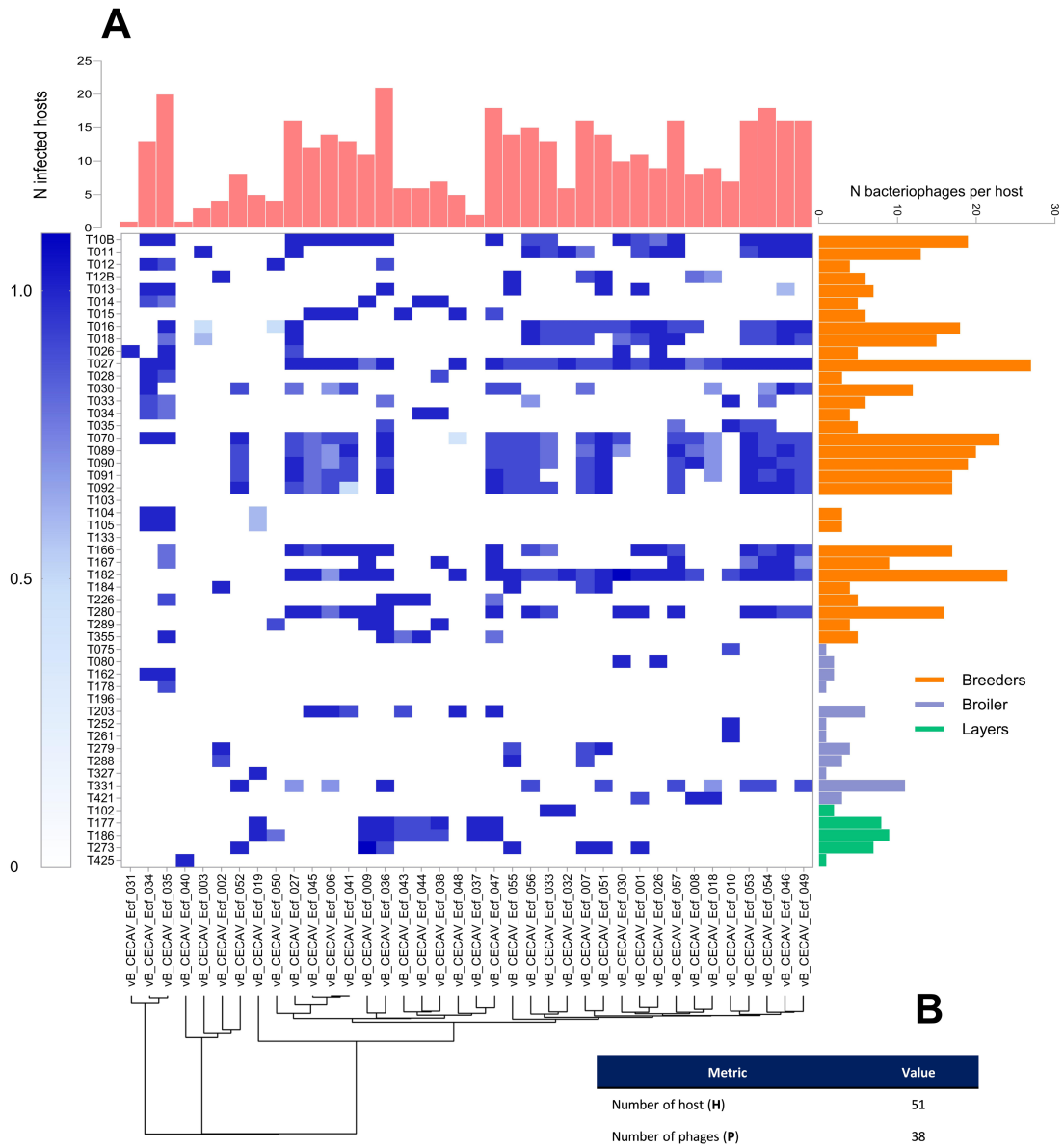
The 38 isolated phages were successfully sequenced and characterized. Combined gene-sharing network analysis and genome-based taxonomic assignment supported the classification of the phage collection into three predicted viral genera: *Saphexavirus* (n = 31; 81.58%), *Efquatrovirus* (n = 4; 10.53%) and *Kochikohdavirus* (n = 3; 7.89%) (Figure 1).

3.2 Phage host range and EOP-based infectivity clustering

EOP analysis was used to determine the productive infectivity of the 38-phage collection against the 51 *E. faecalis* strains. Although phage-host interactions were highly specific, the collection showed broad overall coverage, producing complete lysis in 48 of the 51 tested strains (94.12%) under the conditions evaluated (Figure 2A). The remaining three strains (T103, T133, and T196) exhibited only partial clearing zones, as no individual phage within the collection was capable of producing complete lysis on these hosts. Consequently, these strains were excluded from the EOP analysis. The integrated EOP heatmap and genomic relatedness dendrogram revealed heterogeneous infectivity profiles across the bacterial panel (Figure 2A). Some genomically related phages showed partially overlapping EOP-based profiles, whereas others differed in their infectivity patterns despite close genomic relatedness. Conversely, phages located in distinct genomic branches displayed complementary host-range profiles. This visual pattern was supported by Mantel analysis, which showed a significant positive association between the genotypic distance matrix and the EOP-based Bray–Curtis dissimilarity matrix (r = 0.5215; p = 0.0001). Thus, genomic relatedness was moderately associated with infectivity profiles, but genome-wide similarity alone did not fully explain phage host range, suggesting that genome-wide similarity alone is insufficient to predict host range, reinforcing the relevance of phenotypic screening for accurate cocktail design.

When strains were grouped according to their production origin, phage coverage was consistently high across the different poultry categories. All layer-associated strains were completely lysed by at least one phage (5/5; 100%), while high coverage was also observed among breeder-associated strains (31/33; 93.94%) and broiler-associated strains (12/13; 92.31%).

The interaction metrics further highlighted the structured and specific nature of the phage-host network (Figure 2B). From a total of



Metric	Value
Number of host (**H**)	51
Number of phages (**P**)	38
Number of total interactions (**H x P**)	1,938
Number of positive interactions (**I**)	404
Connectance	0.2085
Host Interactions	
Mean host degree (I/H)	7.9216
Max host degree	27
Min host degree	0
Phage Interactions	
Mean Phage degree (I/P)	10.631
Max Phage degree	21
Min Phage degree	1

FIGURE 2
Host range, interaction metrics and lytic spectrum of the isolated *E. faecalis* phage collection. **(A)** EOP-based host range heatmap showing the infectivity profiles of the 38 bacteriophages against the 51 *E. faecalis* strains. Blue intensity represents normalized EOP values, while white indicates no detectable productive infection. The dendrogram shows clustering of phages according to their EOP-based infectivity profiles. Bar plots indicate the lytic spectrum of each phage and the susceptibility of each bacterial strain, with strains grouped according to poultry production type. **(B)** Summary metrics of the phage-host interaction matrix. **(C)** Distribution of the lytic spectrum of the phage collections.

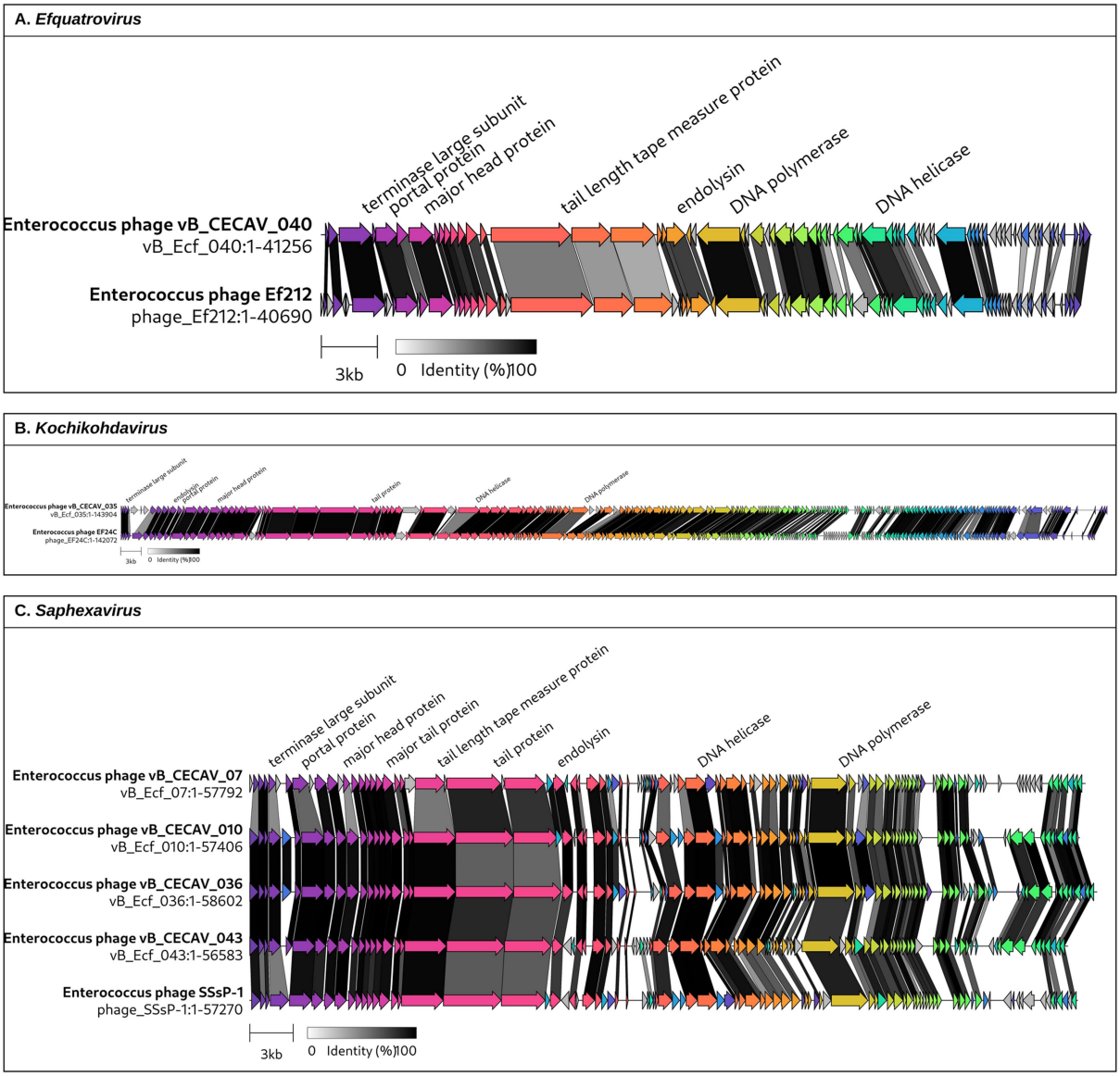


FIGURE 3
Comparative genomic organization of CKT6 phages and RefSeq genomes from the corresponding predicted genera. Arrows represent predicted coding sequences coloured according to functional annotation, and shaded regions indicate homologous genomic regions between phages.

1,938 possible phage-host combinations, 404 were classified as positive productive interactions, resulting in a connectance of 0.2085. This relatively low connectance indicates that, although the collection achieved broad cumulative coverage, individual phage-host interactions remained highly specific. On average, each bacterial strain was infected by 7.92 phages, although host susceptibility varied markedly, ranging from strains with no productive interactions to strains infected by up to 27 phages. Similarly, each phage infected an average of 10.63 bacterial strains, with a wide variation in lytic spectrum among phages.

This variability was also reflected in the distribution of phage lytic spectra (Figure 2C). Most phages showed narrow to intermediate host ranges, whereas a smaller subset displayed broader infectivity profiles. Eleven phages (11/38; 28.95%) showed a broad host range, defined here as productive infection of 15 or more *E. faecalis* strains. Among them, vB_Ecf_035 and vB_Ecf_036 phages exhibited the widest spectra, infecting 21 and 20 strains, respectively, followed by vB_Ecf_047 and vB_Ecf_054, which infected 18 strains each. Collectively, these broad-host-range phages covered 40 of the 51 tested strains (78.43%), supporting their relevance as key candidates for rational multi-phage cocktail design.

3.3 Rational selection of optimized cocktail candidates

The PhageCocktail computational tool enabled the identification of an optimized broad-spectrum combination composed of five (CKT5: vB_Ecf_007, vB_Ecf_010, vB_Ecf_035, vB_Ecf_036, and vB_Ecf_043), six (CKT6: vB_Ecf_007, vB_Ecf_010, vB_Ecf_035, vB_Ecf_036, vB_Ecf_040, and vB_Ecf_043) and seven (CKT7: vB_Ecf_001, vB_Ecf_010, vB_Ecf_035, vB_Ecf_036, vB_Ecf_040, vB_Ecf_043, and vB_Ecf_055) phages, designed to achieve extensive coverage against the total analysed strain collection. CKT7 and CKT5 were able to lyse 88% of the strains (45/51) whereas CKT6 was able

to lyse 92% of the strains (47/51). Mixed-effects logistic regression showed no statistically significant differences among cocktails after Holm correction (all adjusted $p > 0.05$). However, CKT6 showed the most favourable descriptive performance, with approximately 2.26-fold higher odds of complete lysis than CKT5 and 1.33-fold higher odds than CKT7. Given this trend, together with its broader formulation than CKT5 and lower complexity than CKT7, CKT6 was selected as the optimized formulation for downstream characterization and *in vitro* validation.

3.4 Phage genomic characterization and annotation

Full genomic characterization was performed for the six phages selected for the optimized CKT6 cocktail (vB_Ecf_007, vB_Ecf_010, vB_Ecf_035, vB_Ecf_036, vB_Ecf_040, and vB_Ecf_043). All six phages were predicted to have a virulent lifestyle. In addition, no antimicrobial resistance genes, virulence-associated genes, plasmid-related sequences or other undesirable genetic determinants were detected (Table 1).

Genome sizes ranged from 41,256 bp for vB_Ecf_040 to 143,904 bp for vB_Ecf_035, with GC contents between 34.9 and 39.9%. The number of predicted coding sequences varied among phages, from 72 CDS in vB_Ecf_040 to 207 CDS in vB_Ecf_035. Hypothetical proteins represented a high proportion of the predicted proteomes, ranging from 55 to 63% (Table 1).

Genome-based taxonomic assignment classified all six phages within the class *Caudoviricetes*. At the genus level, four phages were assigned to *Saphexavirus* (vB_Ecf_007, vB_Ecf_010, vB_Ecf_036, and vB_Ecf_043) whereas vB_Ecf_035 was assigned to *Kochikohdavirus* and vB_Ecf_040 to *Efquatrovirus* (Table 1).

Comparative genomic visualization using clinker was performed using RefSeq reference genomes from the corresponding predicted genera. The six CKT6 phages displayed modular genome organization, including regions associated with DNA packaging, head and tail morphogenesis, host-cell lysis, and DNA metabolism, with variation observed mainly in structural and tail-associated regions (Figure 3).

Intergenomic similarity analyses using VIRIDIC (Figure 4) and VirClust (Supplementary Figure 2) further supported the genus-level taxonomic assignments obtained through gene-sharing network analysis and taxMyPhage, with nucleotide and proteome-based similarity values consistent with the predicted genus boundaries for each phage.

3.5 Putative depolymerase CDS in CKT6 phages

DePP analysis identified CDS with a predicted probability greater than 90% of encoding putative depolymerases in tail-associated genomic regions of the six CKT6 phages (Table 2). These CDS were annotated as tail proteins, Tal-like tail tip proteins, tail fiber proteins, Dit-like distal tail proteins, minor tail proteins, virion structural proteins, or hypothetical proteins. vB_Ecf_035 contained the highest number of DePP-predicted candidate depolymerase CDS, including a tail protein with lysin activity and a tail fiber protein.

3.6 Morphological and phenotypic characterization of cocktail phages

TEM analysis revealed distinct morphological features among the six bacteriophages, which belong to three different genera (Figure 5). Four phages (vB_Ecf_007, vB_Ecf_010, vB_Ecf_036, and vB_Ecf_043) displayed the characteristic prolate head morphology of the genus *Saphexavirus*, with a long, flexible, non-contractile tail. These phages exhibited elongated capsids with a mean head length ranging from 110.2 ± 1.4 nm (vB_Ecf_036) to 117.3 ± 2.0 nm (vB_Ecf_010) and a mean head width ranging from 41.0 ± 0.3 nm (vB_Ecf_036) to 46.2 ± 1.1 nm (vB_Ecf_007). Tail lengths for *Saphexavirus* phages ranged from 136.9 ± 1.4 nm (vB_Ecf_043) to 147.6 ± 2.2 nm (vB_Ecf_036), with tail widths between 10.8 ± 0.7 nm (vB_Ecf_010) and 12.3 ± 0.4 nm (vB_Ecf_007).

Phage vB_Ecf_035 was classified as a member of the genus *Kochikohdavirus*, exhibiting an isometric icosahedral head

TABLE 1 Genomic and taxonomic characteristics of CKT6 phages.

Feature	vB_Ecf_007	vB_Ecf_010	vB_Ecf_035	vB_Ecf_036	vB_Ecf_040	vB_Ecf_043
Genome size (Kb)	58	57	144	59	41	57
GC content (%)	39.6	39.8	35.9	39.9	34.9	39.8
Coding sequences (CDS)	115	94	207	98	72	94
tRNAs/ pseudogenes	1	1	5	1	0	1
Hypothetical proteins (%)	63	61	56	55	57	62
Accession number	PZ295607.1	PZ295608.1	PZ295609.1	PZ295610.1	PZ400691.1	PZ295606.1
Class	Caudoviricetes	Caudoviricetes	Caudoviricetes	Caudoviricetes	Caudoviricetes	Caudoviricetes
Family	Not defined	Not defined	Herelleviridae	Not defined	Not defined	Not defined
Genus	Saphexavirus	Saphexavirus	Kochikohdavirus	Saphexavirus	Efquatrovirus	Saphexavirus
Predicted lifestyle	Virulent	Virulent	Virulent	Virulent	Virulent	Virulent
AMR/virulence/ plasmid markers	Not detected	Not detected	Not detected	Not detected	Not detected	Not detected

10.3389/fmicb.2026.1924276

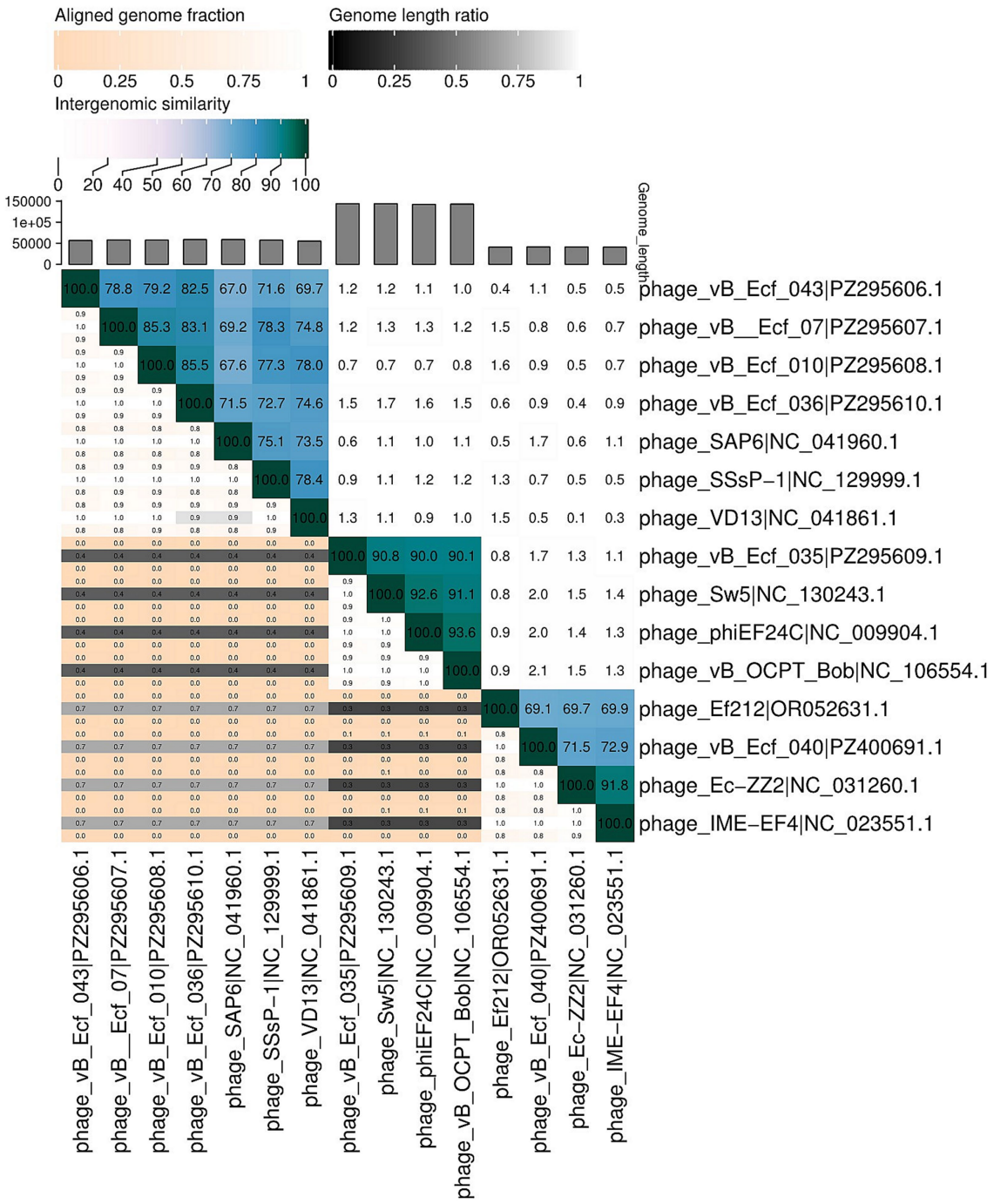


FIGURE 4
Intergenomic similarity heatmap generated by VIRIDIC. The matrix shows pairwise genomic similarity between the studied bacteriophages and RefSeq genomes from the corresponding predicted genera. Values above 70% indicate genus-level relatedness.

(94.0 ± 3.0 nm in diameter) and a contractile tail characteristic of this genus. The extended tail measured 180.2 ± 2.3 nm in length and 19.9 ± 1.7 nm in width. Upon contraction, the tail sheath shortened to 127.5 ± 1.7 nm (29.2% reduction in length, contraction ratio: 1.41×) while increasing in width to 26.8 ± 0.8 nm, reflecting the conformational rearrangement of the tail sheath that drives genome injection into the host cell.

Phage vB_Ecf_040 displayed the morphology characteristic of the genus *Efquatrovirus*, with an isometric icosahedral capsid (66.3 ± 2.1 nm in diameter) and a long, flexible, non-contractile tail (215.8 ± 2.0 nm in length, 10.3 ± 0.8 nm in width). This phage presented the smallest capsid among all six phages and the longest tail.

Regarding pH stability, it ranged between pH 3 and 11, with maximal stability from pH 5 to 9 (Figure 6A). All isolates were completely inactivated at pH 2, indicating high sensitivity to extreme acidic conditions. At pH 3, partial infectivity was retained, with vB_Ecf_010 showing the highest acid tolerance. Viability markedly improved at pH 4, suggesting this value as a lower stability threshold. All phages displayed optimal stability from pH 5 to 9, with complete preservation of infectivity at pH 7

10.3389/fmicb.2026.1924276

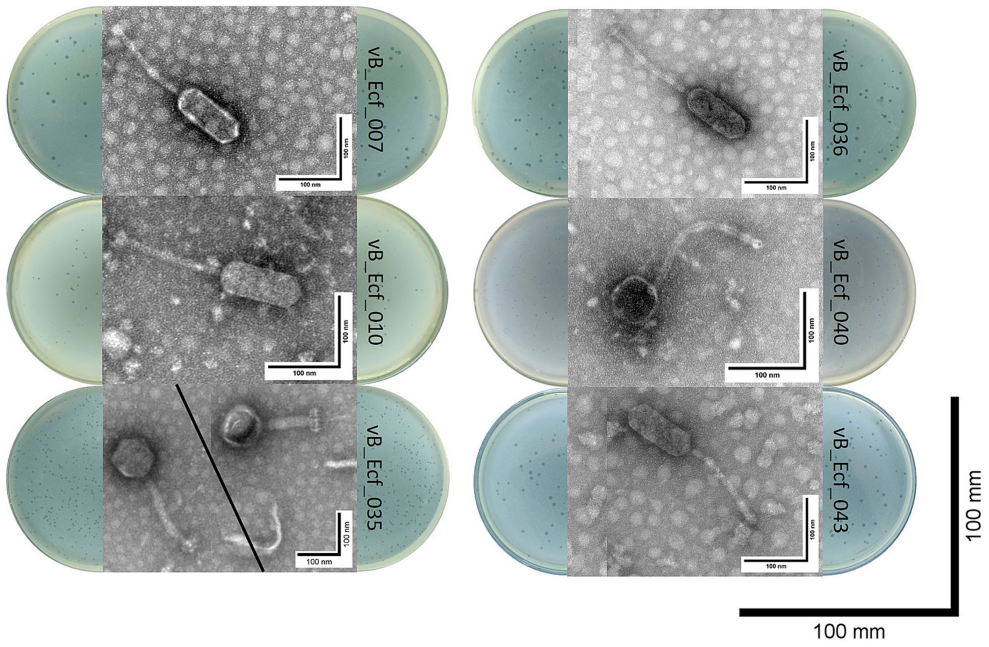


FIGURE 5
Plaque morphology and representative TEM micrographs of the six bacteriophages comprising CKT6. TEM scale bars indicate 100 nm. The scale bar in the bottom-right corner of the Petri dish images indicates 100 mm.

TABLE 2 Predicted depolymerases in CKT6's phages by DePP.

Phage	CDS	Locus	Start	End	Strand	Function	Product
vB_Ecf_007	25	cecavEcc07_025	13.638	17.363	+	Tail	Tail protein
	27	cecavEcc07_027	17.645	20.380	+	Head and packaging	Tail tip protein Tal
vB_Ecf_010	20	cecavEcc010_020	14.253	18.245	+	Tail	Tail protein
	21	cecavEcc010_021	18.258	21.284	+	Head and packaging	Tail tip protein Tal
vB_Ecf_035	32	cecavEcc035_032	25.910	29.095	+	Tail	Tail protein with lysin activity
	33	cecavEcc035_033	29.181	34.658	+	Tail	Tail fiber protein
	34	cecavEcc035_034	34.758	37.169	+	Tail	Tail protein
	44	cecavEcc035_044	44.289	47.753	+	Unknown function	Hypothetical protein
vB_Ecf_036	21	cecavEcc036_021	14.258	18.253	+	Tail	Tail protein
	22	cecavEcc036_022	18.265	21.570	+	Head and packaging	Tail tip protein Tal
vB_Ecf_040	16	cecavEcc040_016	13.409	15.490	+	Tail	Distal tail protein Dit
	17	cecavEcc040_017	15.503	17.815	+	Tail	Minor tail protein
vB_Ecf_043	19	cecavEcc043_019	13.631	17.623	+	Tail	Tail protein
	20	cecavEcc043_020	17.635	20.862	+	Head and packaging	Virion structural protein

and consistently high viability under neutral to mildly alkaline conditions. A gradual decrease was observed at pH 10 and pH 11, although most isolates still retained substantial infectivity. Complete inactivation occurred at pH 12, confirming sensitivity to extreme alkaline conditions.

No significant differences in phage viability were detected between 30 and 60 min of exposure across all temperatures evaluated, therefore, only the results obtained after 60 min of exposure period are presented below (Figure 6B). The thermal stability assays showed that the six-bacteriophages remained stable under refrigeration and frozen storage conditions, with 100% viability at 4 °C and high infectivity at −80 °C and −20 °C. Similarly, viability remained high at 30 °C and 40 °C, indicating good tolerance to ambient and moderately elevated temperatures. A progressive

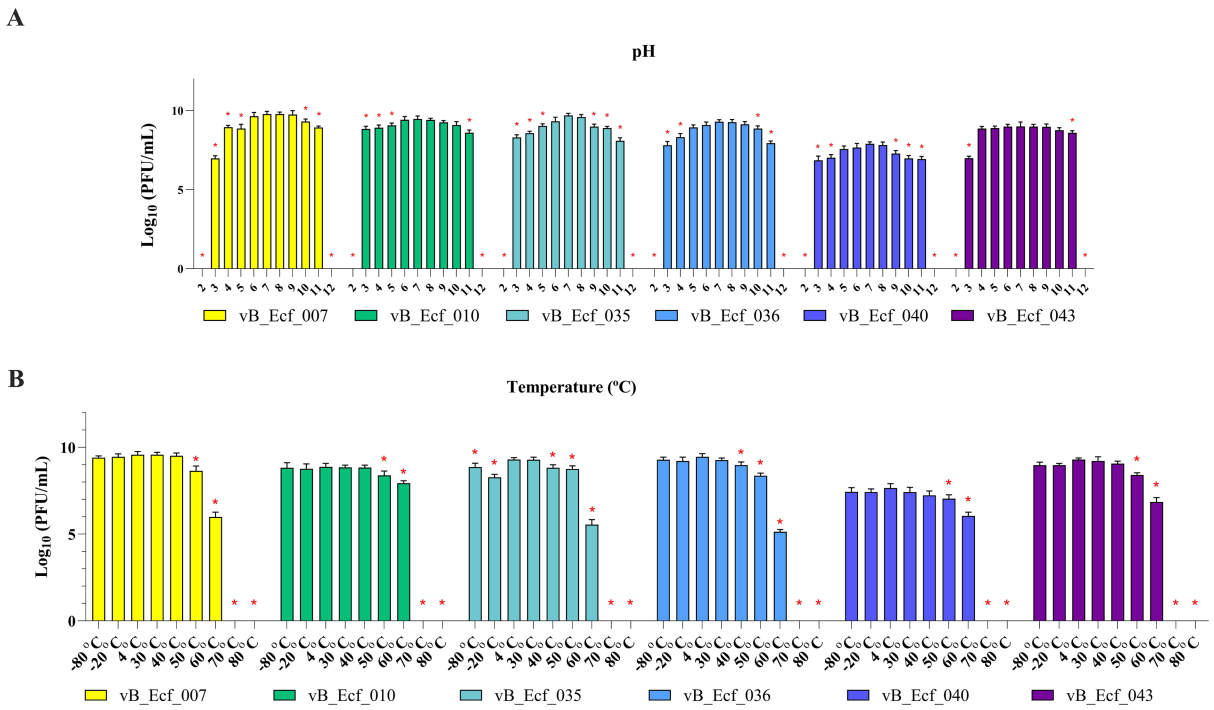


FIGURE 6
pH **(A)** and thermal **(B)** stability of *E. faecalis* bacteriophage isolates. Bar charts showing mean phage viability after 60 min of exposure to each temperature or after 2 h of exposure to each pH condition. with error bars representing standard deviation across biological replicates. Asterisks (*) denote statistically significant differences compared with the control condition (pH 7 for pH stability or 4 °C for thermal stability).

reduction in infectivity was observed from 50 °C onwards. At 50 °C, all isolates retained relatively high viability, with vB_Ecf_010 and vB_Ecf_035 showing the greatest stability. However, at 60 °C, viability declined markedly and varied among isolates, with vB_Ecf_010 displaying the highest residual infectivity and vB_Ecf_036 the lowest. Complete inactivation was observed at 70 °C and 80 °C for all phages. Stability values with the corresponding standard deviations across biological replicates are shown in Figure 6 for both pH and temperature conditions; asterisks (*) indicate statistically significant differences relative to the control condition (pH 7 or 4 °C, respectively).

3.7 One-step growth kinetics and burst size of CKT6 phages

One-step growth curves were determined for the six phages included in the CKT6 cocktail to characterize their latent period and burst size (Figure 7). All six phages displayed a latent period of approximately 20 min, accounting for the 10 min required to enter the exponential growth phase and an additional 10 min allotted to ensure proper attachment, and were followed by a clear rise phase reflecting the release of progeny virions. Burst size varied considerably among phages, ranging from approximately 8 PFU/cell for vB_Ecf_036 to approximately 60 PFU/cell for vB_Ecf_010. Phages vB_Ecf_007, vB_Ecf_035, vB_Ecf_040, and vB_Ecf_043 showed intermediate burst sizes of approximately 12, 11, 9, and 14 PFU/cell, respectively. vB_Ecf_010 was clearly the most productive phage of the cocktail, with a burst size roughly five- to seven-fold higher than the other five phages, while vB_Ecf_036 showed the lowest replicative yield.

3.8 The optimized CKT6 cocktail shows broad *in vitro* activity against clinical poultry isolates

The lytic kinetics of the six phages included in the selected cocktail are shown in Supplementary Figure 3. All phages suppressed or delayed bacterial growth compared with the untreated control, with a clear MOI-dependent effect. Higher MOIs (10 and 1) generally produced faster and stronger reductions in OD, whereas lower MOIs (0.1 and 0.01) were frequently associated with partial bacterial regrowth.

Cocktail CKT6 showed broad lytic activity against the *E. faecalis* strain panel at MOI 1, with 47/51 strains (92.16%) displaying a biphasic kinetic profile characterized by an initial growth phase followed by a marked decrease in normalized OD (Figure 8A). Four strains, T102, T103, T327, and T421, were not effectively controlled by the cocktail and maintained high OD values until the end of the assay. This lack of response was consistent with the absence of productive infectivity of the cocktail components against T103, T327, and T421 in previous EOP assays (see Figure 2), whereas T102 showed only moderate individual phage activity that did not translate into effective suppression in liquid culture. Conversely, T133 and T196 were lysed by the cocktail despite the absence of clearly effective individual activity in the initial screening. To assess whether OD_{600}-based inhibition reflected a reduction in viable bacteria, CFU enumeration was performed in a subset of strains selected as a representative approximation of the different kinetic profiles observed across the collection. These six strains were chosen to illustrate the range of responses identified among the 51 tested isolates, including early (time < 2 h; $n = 22$), middle (time 2-3 h; $n = 22$) and late-phase (time >3 h; $n = 3$) responders, the discordant strains ($n = 2$), and the non-responder strains ($n = 2$) (Figure 8B).

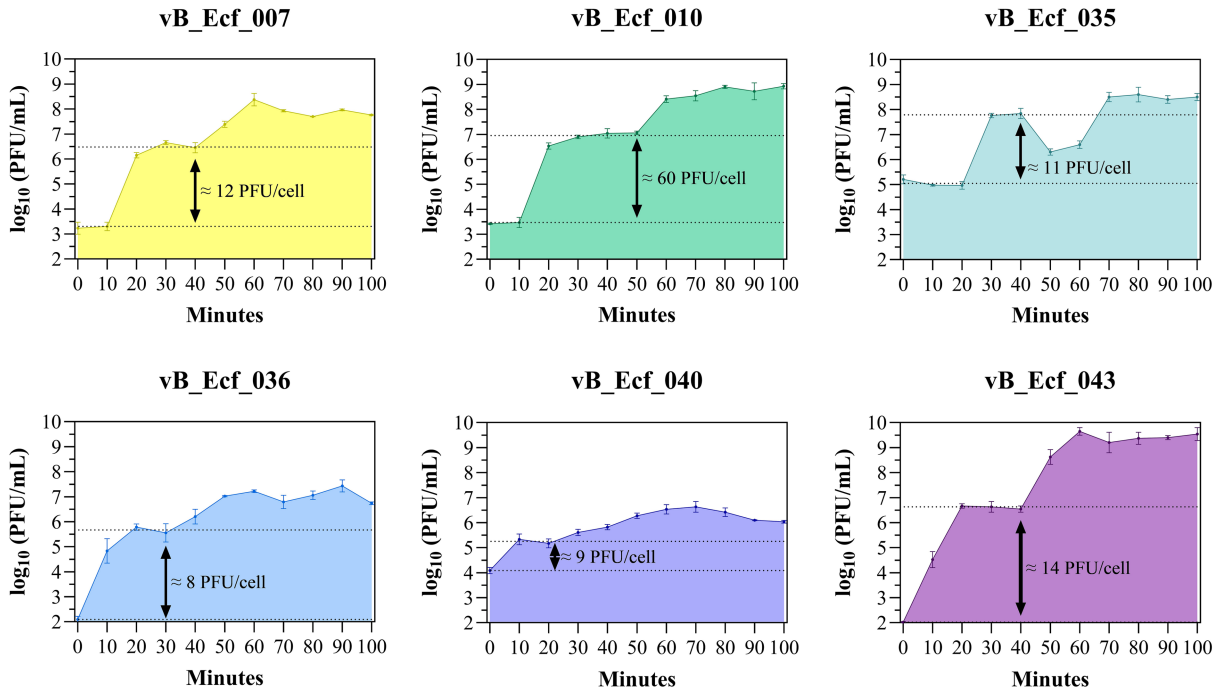


FIGURE 7
One-step growth curves of the six phages selected for the CKT6 cocktail. Phage titers (log_{10} PFU/mL) are shown 100 min post-infection. Dotted lines indicate the initial and final titer plateaus used to estimate burst size (PFU/cell), shown for each phage.

In agreement with the OD_{600} kinetics, CFU enumeration confirmed a marked reduction in viable bacterial counts across the subset of strains tested. CKT6 treatment resulted in no detectable viable recovery for the early-phase responder T27 at 8 h, consistent with a rapid and complete bactericidal effect; counts fell below the limit of detection of the assay (<100 CFU/mL). For T26, classified as a mid-phase responder, a substantial reduction in viable counts was observed, although residual recovery above the detection limit was detected at late time points, suggesting a slower but nonetheless significant lytic effect. The late responder T289 showed a marked reduction in recoverable counts, consistent with the delayed but effective lytic profile observed in the OD_{600} kinetics. The discordant strains T133 and T196, which lacked clearly effective individual phage activity in the initial screening, also exhibited a strong reduction in viable counts upon CKT6 treatment, supporting the ability of the cocktail to control strains with limited individual phage susceptibility, likely through synergistic or complementary activity among cocktail components. In contrast, T102 showed only partial reduction in viable counts, consistent with its poor suppression profile in liquid culture and the moderate individual phage activity previously recorded.

4 Discussion

Enterococcus faecalis is an opportunistic pathogen of One Health relevance. It causes difficult-to-treat human infections and displays both intrinsic and acquired antimicrobial resistance, while poultry-associated enterococci may further contribute to the maintenance and dissemination of resistance determinants along the food chain (Pedersen et al., 2008; Poulsen et al., 2012; Bortolaia et al., 2016; Rodríguez-Lucas and Ladero, 2023; Said et al., 2024). In this context, phages targeting MDR *E. faecalis* from poultry production could provide a complementary strategy to reduce bacterial reservoirs at the animal-production level.

The main contribution of this study is the development of a rational and reproducible approach for phage cocktail design against MDR poultry-associated *E. faecalis*. By coupling extensive field-derived phage isolation with systematic host-range characterization, quantitative infectivity metrics, genomic analysis and computational optimization, this work moves beyond empirical phage selection and provides a data-driven strategy to address the marked heterogeneity of *E. faecalis* populations in poultry production systems.

Here, we report, to our knowledge, one of the largest poultry-associated collections of *E. faecalis* phages described to date, including 38 fully sequenced phages evaluated against 51 clinical poultry isolates. Compared with previous poultry-related studies, which have generally described individual or small numbers of *E. faecalis* phages such as EFC1, EFP6, C-3 and G21-7, the predominance of *Saphexavirus* in our collection (31 out of 38) suggests a recurrent enrichment of this lineage among phages infecting avian-associated *E. faecalis* (Wang and Liu, 2022; Ahmad et al., 2024; Wang et al., 2024; Onaran Acar et al., 2026). However, the description of non-*Saphexavirus* poultry-associated phages indicates that this pattern reflects enrichment rather than exclusivity. These findings position poultry environments as valuable reservoirs of specialized phages for the rational design of targeted biocontrol strategies.

The high functional coverage achieved by the phage collection, with productive infection detected in 94.12% of the tested strains, highlights the value of field-derived phages as candidates for broad-spectrum biocontrol against poultry-associated *E. faecalis*.

10.3389/fmicb.2026.1924276

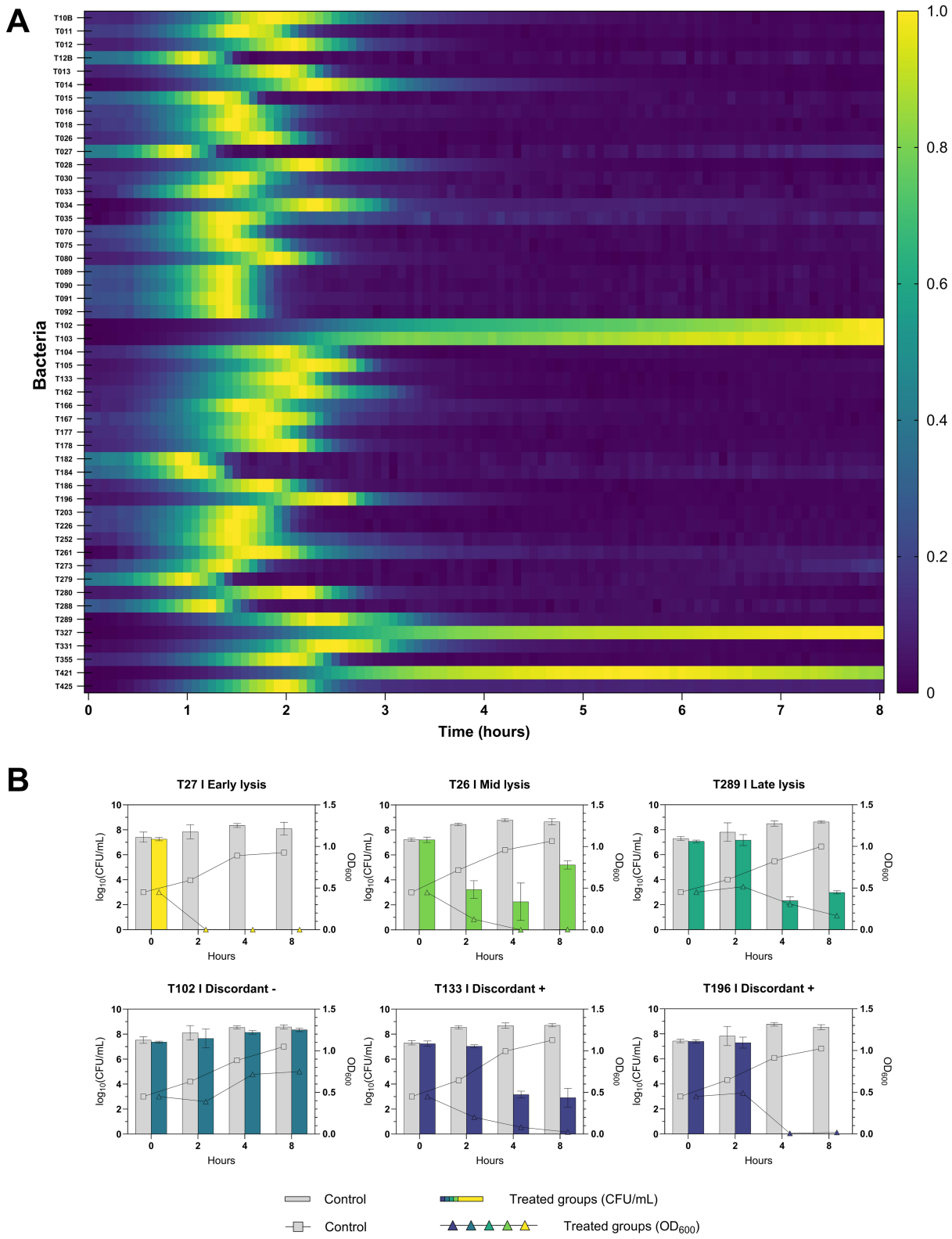


FIGURE 8
Lytic kinetics of cocktail CKT6 and association between phage interaction outcomes and early bacterial suppression. **(A)** Heat map showing normalised OD_{600} kinetics of 51 *Enterococcus* strains exposed to cocktail CKT6 at MOI 1 over 8 h. **(B)** Bacterial counts and OD_{600} profiles in representative strains exposed to CKT6. Bars indicate log_{10} CFU/mL, while superimposed lines indicate OD_{600} values.

Importantly, this coverage was consistently high across poultry production systems, as all layer-associated strains were lysed by at least one phage, while high susceptibility was also observed among breeder and broiler-associated isolates. This is particularly relevant from an applied perspective, as an effective phage-based strategy for poultry production should not be restricted to a single production type, but should retain activity across the bacterial diversity encountered in different epidemiological and management contexts.

In parallel, the genomic diversity of the collection was partially reflected in its infectivity patterns, as Mantel analysis revealed a significant but moderate association between genomic relatedness and EOP-based host-range profiles. Thus, genetically related phages tended to behave similarly, but genome-wide similarity alone did not fully predict infectivity. This is consistent with the concept that phage host range is determined by multiple molecular interactions throughout the infection cycle, particularly receptor recognition, adsorption and post-adsorption compatibility (Hyman and Abedon, 2010; de Jonge et al., 2019). In tailed phages, receptor-binding proteins and tail-associated structures play a central role in host recognition and may strongly influence host specificity even among related phages (Le et al., 2013; Dunne et al., 2021). Therefore, our findings support a cocktail-design strategy that integrates genomic diversity with experimental infectivity data rather than relying solely on phage taxonomy or sequence similarity (Forti et al., 2018; Yang M. et al., 2020; Koncz et al., 2024).

A central aspect of this study was the rational design of the CKT6 cocktail. By integrating EOP-derived HR matrices with computational optimization, a broadly active formulation was obtained while avoiding unnecessary cocktail complexity. The subsequent characterization of the six selected phages further supports their suitability as biocontrol candidates. Their genomes lacked detectable antimicrobial resistance genes, virulence-associated genes or other undesirable genetic determinants, which is an essential safety criterion for phages intended for therapeutic or food-chain applications (Cook and Hynes, 2025). Comparative genomic analysis showed conserved modular organization within the predicted viral genera, while structural and tail-associated regions displayed variability among selected phages. This genomic variability is relevant for cocktail design because tail-associated proteins, including tail fibers and adsorption-related structures, are commonly involved in phage-host interactions and may contribute to differences in host range. The marked variability in burst size observed among the CKT6 phages, ranging from approximately 8 to 60 PFU/cell, further illustrates the heterogeneity in replicative fitness among cocktail components, which may influence their relative contribution to overall bactericidal activity in multi-phage formulations.

Putative depolymerase-associated activities were inferred from plaque morphology and tail-associated annotations. Phage-encoded depolymerases are known to degrade bacterial surface polysaccharides and extracellular polymeric substances, potentially improving phage access to bacteria embedded in structured biofilm matrices (Topka-Bielecka et al., 2021; Guo et al., 2023). The presence of candidate host-recognition and depolymerase-associated proteins is of interest in the context of *E. faecalis*, a species strongly associated with biofilm formation, persistence and increased antimicrobial tolerance (Dale et al., 2017; Lee, 2017; Moryl et al., 2023).

The performance of CKT6 in liquid culture further illustrates the complexity of phage-host interactions and highlights a critical methodological consideration for cocktail efficacy assessment. Although the cocktail showed broad *in vitro* activity, responses varied among strains, indicating that cocktail efficacy cannot be inferred solely from individual phage activity or from genomic similarity. Of note, OD-based kinetic monitoring alone may not fully capture the bactericidal outcome of phage treatment, a sharp decline in optical density is consistent with effective bacterial lysis, but does not exclude the subsequent emergence of phage-resistant variants or resistant subpopulations (Chan et al., 2016; Abedon, 2026), which may repopulate the culture once phage predation pressure is reduced or adsorption becomes limiting (Abedon, 2025), a phenomenon well documented in phage-bacteria co-evolution studies (Lenski and Levin, 1985; Koskella and Brockhurst, 2014).

Conversely, strains that maintained high OD_{600} values throughout the assay cannot be conclusively classified as non-responders without parallel viable counts (Abedon, 2025) since apparent growth could reflect the persistence of a resistant minority that has evaded phage action rather than complete cocktail failure (Chan et al., 2016). These observations underscore the necessity of complementing OD-based kinetics with colony-forming unit (CFU) enumeration to distinguish true bactericidal activity from transient suppression followed by regrowth (Abedon, 2026), and to accurately determine whether apparent lysis reflects a sterilising effect or merely a delay in growth dynamics (Abedon, 2025).

The lack of effective control of strain T102, despite the presence of individually active phages, may reflect mechanisms such as receptor masking, resistant subpopulations, reduced adsorption efficiency or antagonistic interactions under multi-phage conditions. Conversely, the successful lysis of strains T133 and T196, despite limited individual activity, suggests the presence of synergistic effects, potentially involving complementary receptor targeting or enhanced infection dynamics under multi-phage conditions (Hyman and Abedon, 2010; Bertozzi Silva et al., 2016; de Jonge et al., 2019; Wright et al., 2021). In this context, integrating quantitative infectivity data with computational optimization represents a key step toward more predictive cocktail development, particularly because phage combinations may display complementary, neutral or antagonistic interactions depending on the bacterial host and cocktail composition (Forti et al., 2018; Yang Y. et al., 2020; Molina et al., 2022, 2025; Koncz et al., 2024). Future validation studies should therefore incorporate parallel CFU monitoring alongside OD_{600} kinetics to provide a more complete picture of cocktail bactericidal dynamics and to reliably assess long-term suppression efficacy.

Finally, environmental stability assays showed that the selected CKT6 phages-maintained infectivity across a broad range of pH and temperature conditions compatible with many poultry-production settings, supporting their practical potential. However, their sensitivity to extreme acidic conditions indicates that formulation or encapsulation strategies may be required for application routes involving low-pH exposure, such as oral delivery (Malik et al., 2017; Richards and Malik, 2021).

From an applied perspective, CKT6 should therefore be considered a broadly active baseline formulation that could be refined according to circulating *E. faecalis* populations, production type and farm-level epidemiology. This adaptive approach may be particularly important given the strain-level variability observed in this study and the likelihood that no universal phage cocktail will provide sustained efficacy across all poultry-production scenarios. Further validation under biofilm-associated, formulation-relevant and field-like conditions will be essential before considering practical application in poultry production systems. Further studies should extend the evaluation of the selected phages under more complex and

biologically relevant conditions. In particular, their activity against biofilm-associated *E. faecalis*, their interaction with antibiotics in phage-antibiotic combination approaches, and their performance in matrices that better mimic poultry production environments should be investigated. In addition, the emergence of phage-resistant variants and its impact on long-term cocktail efficacy will need to be assessed to refine cocktail composition and improve robustness. These aspects will be essential before considering field-oriented applications.

In conclusion, this study shows that phage cocktail design can evolve from empirical selection toward data-driven and mechanistically informed strategies. By integrating field-derived phage diversity, quantitative infectivity metrics, genomic characterization and computational optimization, we identified a broadly active phage cocktail targeting MDR *E. faecalis* from poultry production. Although further validation under field-relevant conditions is required, our findings highlight the value of functional complementarity and adaptive cocktail design for advancing phage-based approaches at the animal-human interface.

5 Conclusion

This study demonstrates that integrating large-scale EOP-based phage-host interaction profiling with computational optimization provides a framework for the rational and reproducible design of broadly active phage cocktails against MDR *Enterococcus faecalis* from poultry production. The 38-phage collection achieved 94.12% cumulative strain coverage, and the selected six-phage cocktail CKT6 suppressed 92.16% of clinical isolates at MOI 1, with efficacy not fully predictable from individual phage activity. The genomic safety profile, environmental stability, and taxonomic diversity of CKT6 components further support their potential as phage-based biocontrol candidates. Collectively, these findings advance phage cocktail design from empirical selection toward data-driven strategies, and position poultry environments as relevant reservoirs for sourcing specialized phages of One Health significance. Further validation under biofilm-associated and field-relevant conditions remains necessary before practical deployment.

Data availability statement

The datasets presented in this study can be found in the NCBI (https://www.ncbi.nlm.nih.gov) under accession numbers PZ295607.1, PZ295608.1, PZ295609.1, PZ295610.1, PZ400691.1 and PZ295606.1.

Author contributions

JG-L: Data curation, Investigation, Methodology, Software, Writing – original draft, Writing – review & editing, Formal analysis. IG-C: Software, Data curation, Formal analysis, Writing – review & editing. JT-B: Data curation, Writing – review & editing. JS: Validation, Writing – review & editing. PC-G: Validation, Writing – review & editing. SS-N: Conceptualization, Writing – original draft, Formal analysis, Funding acquisition, Project administration, Resources, Supervision, Validation, Writing – review & editing.

Funding

The author(s) declared that financial support was received for this work and/or its publication. This work was supported by project PLEC2023-010275 funded by MICIU/AEI/10.13039/501100011033.

Acknowledgments

The authors would like to thank all members of CECAV for their support, especially, Zaida Carratalà, Sandra Pozo, Mara Sanz and Ester Luengo, for their valuable assistance throughout this work.

Conflict of interest

The author(s) declared that this work was conducted in the absence of any commercial or financial relationships that could be construed as a potential conflict of interest.

Generative AI statement

The author(s) declared that Generative AI was used in the creation of this manuscript. We used the Microsoft 365 Co-Pilot app to review the final manuscript for journal style and content.

Any alternative text (alt text) provided alongside figures in this article has been generated by Frontiers with the support of artificial intelligence and reasonable efforts have been made to ensure accuracy, including review by the authors wherever possible. If you identify any issues, please contact us.

Publisher's note

All claims expressed in this article are solely those of the authors and do not necessarily represent those of their affiliated organizations, or those of the publisher, the editors and the reviewers. Any product that may be evaluated in this article, or claim that may be made by its manufacturer, is not guaranteed or endorsed by the publisher.

Supplementary material

The Supplementary material for this article can be found online at: https://www.frontiersin.org/articles/10.3389/fmicb.2026.1924276/full#supplementary-material

References

Abedon, S. T. (2025). Optical density-based methods in phage biology: Titering, lysis timing, host range, and phage-resistance evolution. *Viruses* 17:1573. doi: 10.3390/v17121573

Abedon, S. T. (2026). Broth optical density-based assessment for phage therapy: turbidity reduction, antibacterial virulence, and time-kill. *Viruses* 18:97. doi: 10.3390/v18010097

Ahmad, S., Leng, Q., Hou, G., Liang, Y., Li, Y., and Qu, Y. (2024). Biological traits and comprehensive genomic analysis of novel *Enterococcus faecalis* bacteriophage EFP6. *Microorganisms* 12:1202. doi: 10.3390/microorganisms12061202

Alrafaie, A. M., Pyrzanowska, K., Smith, E. M., Partridge, D. G., Rafferty, J., Mesnage, S., et al. (2024). A diverse set of Enterococcus-infecting phage provides insight into phage host-range determinants. *Virus Res.* 347:199426. doi: 10.1016/j.virusres.2024.199426

Bertozzi Silva, J., Storms, Z., and Sauvageau, D. (2016). Host receptors for bacteriophage adsorption. *FEMS Microbiol. Lett.* 363:fnw002. doi: 10.1093/femsle/fnw002

Bortolaia, V., Espinosa-Gongora, C., and Guardabassi, L. (2016). Human health risks associated with antimicrobial-resistant enterococci and *Staphylococcus aureus* on poultry meat. *Clin. Microbiol. Infect.* 22, 130–140. doi: 10.1016/j.cmi.2015.12.003

Bouras, G., Nepal, R., Houtak, G., Psaltis, A. J., Wormald, P.-J., and Vreugde, S. (2023). Pharokka: a fast scalable bacteriophage annotation tool. *Bioinformatics* 39:btac776. doi: 10.1093/bioinformatics/btac776

Byappanahalli, M. N., Nevers, M. B., Korajkic, A., Staley, Z. R., and Harwood, V. J. (2012). Enterococci in the environment. *Microbiol. Mol. Biol. Rev.* 76, 685–706. doi: 10.1128/MMBR.00023-12

Bzdil, J., Sladecek, V., Senk, D., Stolar, P., Waicova, Z., Kollertova, N., et al. (2023). Enterococci isolated from one-day-old chickens and their phenotypic susceptibility to antimicrobials in the Czech Republic. *Antibiotics (Basel)* 12:1487. doi: 10.3390/antibiotics12101487

Centers for Disease Control and Prevention (CDC) (2024) Vancomycin-resistant Enterococci (VRE) Basics. Available online at: https://www.cdc.gov/vre/about/index.html (Accessed May 11, 2026).

Chan, B. K., Sistrom, M., Wertz, J. E., Kortright, K. E., Narayan, D., and Turner, P. E. (2016). Phage selection restores antibiotic sensitivity in MDR *Pseudomonas aeruginosa*. *Sci. Rep.* 6:26717. doi: 10.1038/srep26717

Cook, B. W. M., and Hynes, A. P. (2025). Re-evaluating what makes a phage unsuitable for therapy. *NPJ Antimicrob Resist* 3:45. doi: 10.1038/s44259-025-00117-z

Dale, J. L., Nilson, J. L., Barnes, A. M. T., and Dunny, G. M. (2017). Restructuring of *Enterococcus faecalis* biofilm architecture in response to antibiotic-induced stress. *NPJ Biofilms Microbiomes* 3:15. doi: 10.1038/s41522-017-0023-4

De Coster, W., and Rademakers, R. (2023). NanoPack2: population-scale evaluation of long-read sequencing data. *Bioinformatics* 39:btad311. doi: 10.1093/bioinformatics/btad311

de Jonge, P. A., Nobrega, F. L., Brouns, S. J. J., and Dutilh, B. E. (2019). Molecular and evolutionary determinants of bacteriophage host range. *Trends Microbiol.* 27, 51–63. doi: 10.1016/j.tim.2018.08.006

Díaz-Galián, M. V., Vega-Rodríguez, M. A., and Molina, F. (2022). PhageCocktail: An R package to design phage cocktails from experimental phage-bacteria infection networks. *Comput. Methods Prog. Biomed.* 221:106865. doi: 10.1016/j.cmpb.2022.106865

Dunne, M., Prokhorov, N. S., Loessner, M. J., and Leiman, P. G. (2021). Reprogramming bacteriophage host range: design principles and strategies for engineering receptor binding proteins. *Curr. Opin. Biotechnol.* 68, 272–281. doi: 10.1016/j.copbio.2021.02.006

Dupont, H., Friggeri, A., Touzeau, J., Airapetian, N., Tinturier, F., Lobjoie, E., et al. (2011). Enterococci increase the morbidity and mortality associated with severe intra-abdominal infections in elderly patients hospitalized in the intensive care unit. *J. Antimicrob. Chemother.* 66, 2379–2385. doi: 10.1093/jac/dkr308

Forti, F., Roach, D. R., Cafora, M., Pasini, M. E., Horner, D. S., Fiscarelli, E. V., et al. (2018). Design of a broad-range bacteriophage cocktail that reduces *Pseudomonas aeruginosa* biofilms and treats acute infections in two animal models. *Antimicrob. Agents Chemother.* 62, e02573–e02517. doi: 10.1128/aac.02573-17

Garcia-Llorens, J., Monroy, I., Torres-Boncompte, J., Soriano, J. M., Catalá-Gregori, P., and Sevilla-Navarro, S. (2025). Tracking the prevalence of antibiotic resistance in *Enterococcus* within the Spanish poultry industry: insights from a one health approach. *Antibiotics* 14:16. doi: 10.3390/antibiotics14010016

Gilchrist, C. L. M., and Chooi, Y.-H. (2021). Clinker & clustermap.Js: automatic generation of gene cluster comparison figures. *Bioinformatics* 37, 2473–2475. doi: 10.1093/bioinformatics/btab007

Guo, Z., Liu, M., and Zhang, D. (2023). Potential of phage depolymerase for the treatment of bacterial biofilms. *Virulence* 14:2273567. doi: 10.1080/21505594.2023.2273567

Hyman, P., and Abedon, S. T. (2010). Bacteriophage host range and bacterial resistance. In: Advances in Applied Microbiology. Vol. 70. Laskin A. I., Sariaslani S., and Gadd G. M. (Eds.), San Diego, CA, USA: Academic Press. p. 217–248.

Jang, H. B., Bolduc, B., Zablocki, O., Kuhn, J. H., Roux, S., Adriaenssens, E. M., et al. (2019). Taxonomic assignment of uncultivated prokaryotic virus genomes is enabled by gene-sharing networks. *Nat. Biotechnol.* 37, 632–639. doi: 10.1038/s41587-019-0100-8

Jung, A., Chen, L. R., Suyemoto, M. M., Barnes, H. J., and Borst, L. B. (2018). A review of *Enterococcus cecorum* infection in poultry. *Avian Dis.* 62, 261–271. doi: 10.1637/11825-030618-Review.1

Kerek, Á., Szabó, Á., and Jerzsele, Á. (2024). Antimicrobial susceptibility profiles of commensal Enterococcus spp. isolates from chickens in hungarian poultry farms between 2022 and 2023. *Antibiotics* 13:1194. doi: 10.3390/antibiotics13121194

Kolmogorov, M., Yuan, J., Lin, Y., and Pevzner, P. A. (2019). Assembly of long, error-prone reads using repeat graphs. *Nat. Biotechnol.* 37, 540–546. doi: 10.1038/s41587-019-0072-8

Koncz, M., Stirling, T., Mehdi, H. H., Méhi, O., Eszenyi, B., Asbóth, A., et al. (2024). Genomic surveillance as a scalable framework for precision phage therapy against antibiotic-resistant pathogens. *Cell* 187, 5901–5918.e28. doi: 10.1016/j.cell.2024.09.009

Koskella, B., and Brockhurst, M. A. (2014). Bacteria-phage coevolution as a driver of ecological and evolutionary processes in microbial communities. *FEMS Microbiol. Rev.* 38, 916–931. doi: 10.1111/1574-6976.12072

Kutter, E. (2009). Phage host range and efficiency of plating. In: Bacteriophages: Methods and Protocols, Volume 1: Isolation, Characterization, and Interactions. Methods in Molecular Biology. Clokie, M. R. and Kropinski, A. M. Eds. Vol. 501. Totowa, NJ, USA: Humana Press. p. 141–149.

Kutter, E., De Vos, D., Gvasalia, G., Alavidze, Z., Gogokhia, L., Kuhl, S., et al. (2010). Phage therapy in clinical practice: treatment of human infections. *Curr. Pharm. Biotechnol.* 11, 69–86. doi: 10.2174/138920110790725401

Lavilla, M., Domingo-Calap, P., Sevilla-Navarro, S., and Lasagabaster, A. (2023). Natural killers: opportunities and challenges for the use of bacteriophages in microbial food safety from the one health perspective. *Foods* 12:552. doi: 10.3390/foods12030552

Le, S., He, X., Tan, Y., Huang, G., Zhang, L., Lux, R., et al. (2013). Mapping the tail fiber as the receptor binding protein responsible for differential host specificity of *Pseudomonas aeruginosa* bacteriophages PaP1 and JG004. *PLoS One* 8:e68562. doi: 10.1371/journal.pone.0068562

Lee, Y. (2017). Biofilm formation and antimicrobial resistance in Enterococcus. *Infect Chemother* 49, 236–237. doi: 10.3947/ic.2017.49.3.236

Lee, J. Y., Kong, M., Oh, J., Lim, J., Chung, S. H., Kim, J.-M., et al. (2021). Comparative evaluation of Nanopore polishing tools for microbial genome assembly and polishing strategies for downstream analysis. *Sci. Rep.* 11:20740. doi: 10.1038/s41598-021-00178-w

Lenski, R. E., and Levin, B. R. (1985). Constraints on the coevolution of bacteria and virulent phage: a model, some experiments, and predictions for natural communities. *Am. Nat.* 125, 585–602. doi: 10.1086/284364

Li, H. (2018). Minimap2: pairwise alignment for nucleotide sequences. *Bioinformatics* 34, 3094–3100. doi: 10.1093/bioinformatics/bty191

Li, X., Zhao, M., Zhang, L., Sun, G., Duan, X., and Chen, G. (2026). Characteristics, whole genome analysis of a virulent phage from avian-derived Enterococcus faecalis and its application in poultry product processing safety. *Microorganisms* 14:490. doi: 10.3390/microorganisms14020490

Magill, D. J., and Skvortsov, T. A. (2023). DePolymerase predictor (DePP): a machine learning tool for the targeted identification of phage depolymerases. *BMC Bioinformatics* 24:208. doi: 10.1186/s12859-023-05341-w

Malik, D. J., Sokolov, I. J., Vinner, G. K., Mancuso, F., Cinquerrui, S., Vladisavljević, G. T., et al. (2017). Formulation, stabilisation and encapsulation of bacteriophage for phage therapy. *Adv. Colloid Interf. Sci.* 249, 100–133. doi: 10.1016/j.cis.2017.05.014

Martinez-Laorden, A., Arraiz-Fernandez, C., and Gonzalez-Fandos, E. (2023). Identification and characterisation of antimicrobial resistance of *Enterococcus* spp. isolated from pork and poultry meat. *Int. J. Food Sci. Technol.* 58, 4455–4463. doi: 10.1111/ijfs.16562

McNair, K., Zhou, C., Dinsdale, E. A., Souza, B., and Edwards, R. A. (2019). PHANOTATE: a novel approach to gene identification in phage genomes. *Bioinformatics* 35, 4537–4542. doi: 10.1093/bioinformatics/btz265

Millard, A., Denise, R., Lestido, M., Nicholas, M. T., Webster, D., Turner, D., et al. (2025). taxMyPhage: automated taxonomy of dsDNA phage genomes at the genus and species level. *PHAGE: Therapy Applic. Res.* 6, 5–11. doi: 10.1089/phage.2024.0050

Mirzaei, M. K., and Nilsson, A. S. (2015). Isolation of phages for phage therapy: a comparison of spot tests and efficiency of plating analyses for determination of host range and efficacy. *PLoS One* 10:e0118557. doi: 10.1371/journal.pone.0118557

Molina, F., Menor-Flores, M., Fernández, L., Vega-Rodríguez, M. A., and García, P. (2022). Systematic analysis of putative phage-phage interactions on minimum-sized phage cocktails. *Sci. Rep.* 12:2458. doi: 10.1038/s41598-022-06422-1

Molina, F., Menor-Flores, M., and Vega-Rodríguez, M. A. (2025). SocialViruses: integrating quantitative phage–bacteria and phage–phage interaction networks for rational cocktail design. *Bioinformatics Adv.* 5:vbaf239. doi: 10.1093/bioadv/vbaf239

Morishita, TY. (2025). Enterococcosis in poultry. MSD veterinary manual. Available online at: https://www.msdvetmanual.com/poultry/enterococcosis/enterococcosis-in-poultry (Accessed May 11, 2026).

Moryl, M., Różalski, A., and Torzewska, A. (2023). How do phages disrupt the structure of *Enterococcus faecalis* biofilm? *Int. J. Mol. Sci.* 24:17260. doi: 10.3390/ijms242417260

Nayfach, S., Camargo, A. P., Schulz, F., Eloe-Fadrosh, E., Roux, S., and Kyrpides, N. C. (2021). CheckV assesses the quality and completeness of metagenome-assembled viral genomes. *Nat. Biotechnol.* 39, 578–585. doi: 10.1038/s41587-020-00774-7

Nielsen, S. S., Bicout, D. J., Calistri, P., Canali, E., Drewe, J. A., Garin-Bastuji, B., et al. (2022). Assessment of listing and categorisation of animal diseases within the framework of the animal health law (regulation (EU) no 2016/429): antimicrobial-resistant *Enterococcus faecalis* in poultry. *EFSA J.* 20:e07127. doi: 10.2903/j.efsa.2022.7036

Onaran Acar, B., Erdinç, A. N., Yildiz, T., and Ayaz, N. D. (2026). Novel *Enterococcus* phages identified through comprehensive screening to control contamination in chicken meat. *J. Sci. Food Agric.* 106, 5671–5679. doi: 10.1002/jsfa.70607

Panteleev, V., Kulbachinskiy, A., and Gelfenbein, D. (2025). Evaluating phage lytic activity: from plaque assays to single-cell technologies. 16:1659093. *Front. Microbiol.* doi: 10.3389/fmicb.2025.1659093

Pedersen, T. B., Olsen, J. E., and Bisgaard, M. (2008). Persistence of Salmonella Senftenberg in poultry production environments and investigation of its resistance to desiccation. 37, 421–427. doi: 10.1080/03079450802216561

Poulsen, L. L., Bisgaard, M., Son, N. T., Trung, N. V., An, H. M., and Dalsgaard, A. (2012). *Enterococcus faecalis* clones in poultry and in humans with urinary tract infections, Vietnam. *Emerg. Infect. Dis.* 18, 1096–1100. doi: 10.3201/eid1807.111754

R Core Team. (2025). R: A language and environment for statistical computing (Version 4.5.3). R Foundation for Statistical Computing. Available online at: https://www.R-project.org/

Reynolds, D. L., Hille, M. M., and Jia, B. (2025). Review of *Enterococcus faecalis* infections of poultry. *Avian Dis. American Asso. Avian Pathologists*. 68, 412–420. doi: 10.1637/aviandiseases-D-24-00084

Richards, K., and Malik, D. J. (2021). Bacteriophage encapsulation in pH-responsive core-shell capsules as an animal feed additive. *Viruses* 13:1131. doi: 10.3390/v13061131

Rodríguez-Lucas, C., and Ladero, V. (2023). Enterococcal phages: food and health applications. *Antibiotics* 12:842. doi: 10.3390/antibiotics12050842

Said, MS, Tirthani, E, and Lesho, E (2024) Enterococcus infections. Available online at: https://www.ncbi.nlm.nih.gov/books/NBK567759/ (Accessed May 11, 2026).

Seemann, TA (2016) ABRicate: mass screening of contigs for antibiotic resistance genes. Available online at: https://github.com/tseemann/abricate (Accessed May 14, 2026).

Shang, J., Peng, C., Liao, H., Tang, X., and Sun, Y. (2023b). PhaBOX: a web server for identifying and characterizing phage contigs in metagenomic data. *Bioinformatics Adv.* 3:vbad101. doi: 10.1093/bioadv/vbad101

Shang, J., Tang, X., and Sun, Y. (2023a). PhaTYP: predicting the lifestyle for bacteriophages using BERT. *Brief. Bioinform.* 24:bbac487. doi: 10.1093/bib/bbac487

Shannon, P., Markiel, A., Ozier, O., Baliga, N. S., Wang, J. T., Ramage, D., et al. (2003). Cytoscape: a software environment for integrated models of biomolecular interaction networks. *Genome Res.* 13, 2498–2504. doi: 10.1101/gr.1239303

Stępień-Pyśniak, D., Marek, A., Banach, T., Adaszek, Ł., Pyzik, E., Wilczyński, J., et al. (2016). Prevalence and antibiotic resistance of Enterococcus strains isolated from poultry. *Acta Vet. Hung.* 64, 148–163. doi: 10.1556/004.2016.016

Topka-Bielecka, G., Dydecka, A., Necel, A., Bloch, S., Nejman-Faleńczyk, B., Węgrzyn, G., et al. (2021). Bacteriophage-derived depolymerases against bacterial biofilm. *Antibiotics* 10:175. doi: 10.3390/antibiotics10020175

Torres-Boncompte, J., Gómez-Cano, I. S., Garcia-Llorens, J., Soriano, J. M., Catalá-Gregori, P., and Sevilla-Navarro, S. (2025). Characterization and therapeutic potential of newly isolated bacteriophages targeting the most common Salmonella serovars in Europe. *Sci. Rep.* 15:10872. doi: 10.1038/s41598-025-95398-9

Uyttebroek, S., Chen, B., Onsea, J., Ruythooren, F., Debaveye, Y., Devolder, D., et al. (2022). Safety and efficacy of phage therapy in difficult-to-treat infections: a systematic review. *Lancet Infect. Dis.* 22, e208–e220. doi: 10.1016/S1473-3099(21)00612-5

Vaser, R., Sović, I., Nagarajan, N., and Šikić, M. (2017). Fast and accurate de novo genome assembly from long uncorrected reads. *Genome Res.* 27, 737–746. doi: 10.1101/gr.214270.116

Wang, Q., and Liu, N. (2022). Complete genome analysis of bacteriophage EFC1 infecting *Enterococcus faecalis* from chicken. *Arch. Microbiol.* 204:413. doi: 10.1007/s00203-022-02838-5

Wang, T., Zhang, L., Zhang, Y., Tong, P., Ma, W., Wang, Y., et al. (2024). Isolation and identification of specific *Enterococcus faecalis* phage C-3 and G21-7 against avian pathogenic Escherichia coli and its application to one-day-old geese. *Front. Microbiol.* 15:1385860. doi: 10.3389/fmicb.2024.1385860

Wright, R. C. T., Friman, V.-P., Smith, M. C. M., and Brockhurst, M. A. (2021). Functional diversity increases the efficacy of phage combinations. *Microbiology (N Y)* 167:1110. doi: 10.1099/mic.0.001110

Yang, M., Liang, Y., Huang, S., Zhang, J., Wang, J., Chen, H., et al. (2020). Isolation and characterization of the novel phages vB_VpS_BA3 and vB_VpS_CA8 for lysing *Vibrio parahaemolyticus*. *Front. Microbiol.* 11:256. doi: 10.3389/fmicb.2020.00259

Yang, Y., Shen, W., Zhong, Q., Chen, Q., He, X., Baker, J. L., et al. (2020). Development of a bacteriophage cocktail to constrain the emergence of phage-resistant *Pseudomonas aeruginosa*. *Front. Microbiol.* 11:327. doi: 10.3389/fmicb.2020.00327

Yukgehnaish, K., Rajandas, H., Parimannan, S., Manickam, R., Marimuthu, K., Petersen, B., et al. (2022). PhageLeads: rapid assessment of phage therapeutic suitability using an ensemble machine learning approach. *Viruses* 14:342. doi: 10.3390/v14020342